Cedar Lake, Wisconsin - Limnological response to alum treatment: 2020 interim report

17 December 2020

University of Wisconsin – Stout
Sustainability Sciences Institute - Center for Limnological Research and Rehabilitation
Department of Biology
123E Jarvis Hall
Menomonie, Wisconsin 54751
715-338-4395
jamesw@uwstout.edu

Harmony Environmental
516 Keller Ave S
Amery, Wisconsin 54001
715-268-9992
harmonyenv@amerytel.net

Executive Summary

- In 2020, ~ one year after the second partial Al treatment (2019), mean summer (JUL-early OCT) concentrations of surface total phosphorus P and chlorophyll increased above target WQ goals to 0.050 mg/L and 28 µg/L, respectively. Peak total P and chlorophyll in early September were 0.074 mg/L and 65 µg/L respectively.

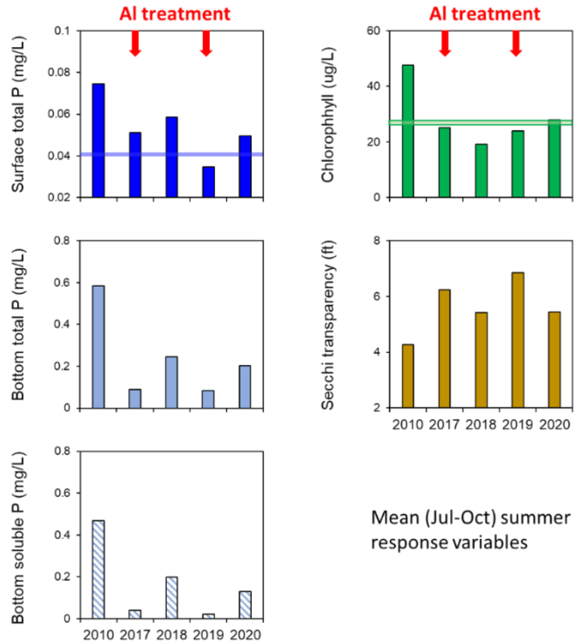

- Increases in surface total P and chlorophyll coincided with hypolimnetic P accumulation as a result of internal P loading, indicating that sediment diffusive P flux overwhelmed Al floc binding capacity. Bottom P concentration peaks exceeded 0.50 mg/L in 2020.
- Although mean limnological response variables were more impaired in 2020, relative to 2019, means in surface total P, bottom total P and SRP, chlorophyll, and Secchi transparence were still 34%, 65%, 72%, 41%, and 27% improved compared to the pretreatment mean.
- Total aluminum concentrations in the upper 5-cm sediment layer were less than target projected (theoretical) Al concentrations of 42 g/m^2 at the 20-25 ft depth contour and 56 g/m^2 at some stations in 2020. Some of the alum may have mixed downward below the 5-cm sediment section and was, thus, not measured. So, lower added Al recovery (i.e., the added alum) may be attributed to sectioning only the upper 5-cm sediment layer. In addition, the Al floc may have moved or become redistributed and spread during or after application by wind activity and water currents. Al floc movement during settling is not uncommon and has been reported to occur in other alum treatments.
- It is recommended the Lake District strongly consider applying all the 3rd scheduled Al application to the > 25-ft depth contour in 2021. As 2020, most of the hypolimnetic

anoxia and P accumulation was confined to depths > 7.5 m or 25 ft, arguing for concentrating the third partial dose to only this area. Without increasing costs, Al application to depths > 25 ft only in 2021 would result in an Al concentration of 50 g/m^2 versus 26 g/m^2, leading to a theoretical total Al concentration of > 90 g/m^2 in this area after the third treatment. The success of this 2021 application in maintaining target limnological goals will be assessed (monitoring and adaptive management) and information gleaned will be used to adjust the application timing, treatment area, and Al dosage of the fourth and fifth treatments.

Objectives

Multiple Al applications over a period of 10-12 years are planned for Cedar Lake in order to control internal phosphorus loading. It is critical to conduct post-treatment monitoring of water and sediment chemistry to document the trajectory of water quality improvement during rehabilitation to make informed decisions regarding adjusting management to meet future water quality goals. Post-treatment monitoring included field and laboratory research to document changes in 1) hydrology and watershed phosphorus (P) loading, 2) the P budget and lake water quality, 3) binding of sediment mobile P fractions that have contributed to internal P loading by alum, and 4) rates of diffusive P flux from the sediment under anaerobic conditions. Overall, lake water quality is predicted to respond to watershed and internal P loading reduction with lower surface concentrations of total P and chlorophyll concentrations throughout the summer, lower bloom frequency of nuisance chlorophyll levels, and higher water transparency. Multiple Al applications between 2017 and 2029 should result in the binding of iron-bound P and substantial reduction in diffusive P flux from sediments under anaerobic conditions (i.e., internal P loading). The first alum application occurred in late June 2017. The Al concentration was 20 g/m^2 for sediment located within the 20-25 ft depth contour and 26 g/m^2 for sediment located at depths > 25 ft. The second alum application occurred during 11-22 June 2019 and Al concentrations ranged between 22 g/m^2 within the 20-25 ft depth contour and ~ 28 g/m^2 for depths > 25 ft. Current combined Al application of 42 g/m^2 and 54 g/m^2 to the two depth zones represents ~ 42% of the target Al doses of 100 g/m^2 and 130 g/m^2. The objectives of this interim report were to describe the 2020 limnological and sediment variable response to these alum treatments in

Cedar Lake. Limnological monitoring is being used in conjunction with an adaptive management approach to gauge lake response and the need, if any, to adjust Al dose or application strategy.

Methods

Watershed loading and lake monitoring

A gauging station was established on Horse Creek above Cedar Lake at 10^{th} Ave for concentration, loading, and flow determination between May and October 2020 (Fig. 1). Grab samples were collected biweekly at the 10^{th} Ave gauging station for chemical analysis. Water samples were analyzed for total P, and soluble reactive P (SRP) using standard methods (APHA 2011). Summer tributary P loading was calculated using the computer program FLUX.

The deep basin water quality station WQ 2 was sampled biweekly between May and October 2020 (Fig. 1). An integrated sample over the upper 2-m was collected for analysis of total P, SRP, and chlorophyll a. An additional discrete sample was collected within 0.5 m of the sediment surface for analysis of total and SRP. Secchi transparency and in situ measurements (temperature, dissolved oxygen, pH, and conductivity) were collected on each date using a YSI 6600 sonde (Yellow Springs Instruments) that was calibrated against dissolved oxygen Winkler titrations (APHA 2011) and known buffer solutions.

Sediment chemistry

Sediment characteristics. A sediment core was collected in August 2020 at WQ 2 (Fig. 1) for determination of vertical profiles of various sediment characteristics and phosphorus fractions (see Analytical methods below). The sediment core was sectioned at 1-cm intervals between 0 and 10 cm and at 2-cm intervals below the 10-cm depth for determination of moisture content, wet and dry bulk density, loss-on-ignition organic matter, loosely-bound P, iron-bound P, labile organic P, and aluminum-bound P.

Laboratory-derived diffusive phosphorus flux from sediments under anaerobic conditions.

Anaerobic diffusive P fluxes were measured from intact sediment cores collected at stations shown in Figure 1 in August 2020. One sediment core was collected at each station to monitor alum treatment effectiveness after application. The sediment incubation systems were placed in a darkened environmental chamber and incubated at 20 C for up to 5 days. The incubation temperature was set to a standard temperature for all stations for comparative purposes. The oxidation-reduction environment in each system was controlled by gently bubbling nitrogen through an air stone placed just above the sediment surface to maintain anaerobic conditions.

Water samples for SRP were collected from the center of each system using an acid-washed syringe and filtered through a 0.45 µm membrane syringe filter (Nalge). The water volume removed from each system during sampling was replaced by addition of filtered lake water preadjusted to the proper oxidation-reduction condition. These volumes were accurately measured for determination of dilution effects. Rates of P release from the sediment (mg/m^2 d) were calculated as the linear change in mass in the overlying water divided by time (days) and the area (m^2) of the incubation core liner. Regression analysis was used to estimate rates over the linear portion of the data.

Analytical methods. A known volume of sediment was dried at 105 ^oC for determination of moisture content, wet and dry bulk density, and burned at 550 ^oC for determination of loss-on-ignition organic matter content (Avnimelech et al. 2001, Håkanson and Jansson 2002). Phosphorus fractionation was conducted according to Hieltjes and Lijklema (1980), Psenner and Puckso (1988), and Nürnberg (1988) for the determination of ammonium-chloride-extractable P (loosely-bound P), bicarbonate-dithionite-extractable P (i.e., iron-bound P), and sodium hydroxide-extractable P (i.e., aluminum-bound P).

The loosely-bound and iron-bound P fractions are readily mobilized at the sediment-water interface as a result of anaerobic conditions that lead to desorption of P from sediment and diffusion into the overlying water column (Mortimer 1971, Boström et al. 1982, Boström 1984, Nürnberg 1988). The sum of the loosely-bound and iron-bound P fraction represents redox-sensitive P (i.e., the P fraction that is active in P release under anaerobic and reducing conditions) and will be referred to as ***redox-P***. Aluminum-bound P reflects P bound to the Al floc after aluminum sulfate application and its chemical transformation to aluminum hydroxide ($Al(OH)_3$).

Summary of Results

Hydrology and phosphorus loading

On an annual basis, precipitation in 2020 was average at ~32 inches compared to the ~ 33-inch average since 1980 (Fig. 2). Monthly precipitation exceeded the long-term average in June and July (Fig. 3). In contrast, monthly precipitation was less than the long-term average in August and September 2020.

Horse Creek summer flow exhibited major peaks between May and July in conjunction with storms (Fig. 4). Peak flow in mid-May, late June, and late July were associated with daily precipitation (measured at Amery, Wisconsin) that approached or exceeded 2 inches. The greatest daily precipitation event occurred in late July at nearly 3 inched. Flows subsided during a period of lower precipitation in August through September. Horse Creek mean summer (May-October) daily flow was high relative to other years at 0.86 m^3/s in 2020 (Fig. 5) even though summer precipitation at Amery Wisconsin was moderate. This pattern could be related to the occurrence of several high intensity storms that caused higher than normal flow peaks.

Total P concentrations in Horse Creek were elevated in conjunction with peak flows in late May and late June 2020 (Fig. 6). They declined during the lower flow period between August and early October. Soluble reactive P concentrations increased to a maximum during the late June peak in the hydrograph.

Concentration-flow relationships in 2020 were generally like those observed historically (Fig. 7). Flow-averaged summer (May through October) total P and SRP in 2020 were 0.083 mg/L and 0.033 mg/L (Table 1). The flow-averaged SRP concentration accounted for ~ 40% of the total P in 2020. Summer total P and SRP loadings from Horse Creek were 6.14 and 2.35 kg/d (Table 1), respectively, in 2020, higher than loads estimates during research in 2009-11 and 2017-19. This pattern may be attributable to several high intensity storm periods (daily precipitation ~ 2-3 inches) that caused excessive watershed runoff and P loading.

Table 1. Mean summer (May-October) constituent concentrations and loading for the Horse Creek inflow station at 10th Ave.

Year	Variable	TSS	Total P	SRP
2010	Concentration (mg/L)		0.089	0.031
	Load (kg/d)		4.18	1.42
2017	Concentration (mg/L)	15.2	0.084	0.034
	Load (kg/d)	767.8	4.26	1.71
2018	Concentration (mg/L)	16.5	0.100	0.039
	Load (kg/d)	549	3.36	1.28
2019	Concentration (mg/L)	10.6	0.083	0.035
	Load (kg/d)	524	4.07	1.72
2020	Concentration (mg/L)		0.083	0.033
	Load (kg/d)		6.14	2.35

Lake limnological response

Cedar Lake was strongly stratified between early June and late-August 2020 (Fig. 8). Water column cooling resulted in progressive epilimnetic expansion between late July and August 2020. Complete water column mixing and turnover occurred in early-September 2020. Bottom water anoxia was established between early June and late-August 2020. Anoxia extended to about 6.5 m in mid-July 2020 compared to ~ 5.5 m in 2010. However, the vertical extent of anoxia was otherwise confined to depths > 7 m. In particular, the extent of bottom anoxia was reduced substantially in conjunction with the period of epilimnetic expansion between late July through August.

Prior to the initiation of alum treatments, total P and SRP concentrations increased in the bottom waters in conjunction with the development of hypolimnetic anoxia in early June, suggesting the beginning of internal P loading (Fig. 9). Bottom water P concentrations declined as a result of the June 2019 alum treatment and remained low and nominal throughout the summer. However, P concentrations in the bottom waters increased to ~ 0.51 mg/L total P and 0.44 mg/L soluble P in early August, suggesting sediment diffusive P flux (i.e., internal P loading) was beginning to overwhelm Al floc binding efficiency. A similar pattern occurred in 2018, after the first (2017) Al application. Nevertheless, concentration peaks were much lower and shorter-lived in 2020 compared to those in 2010 (i.e., > 1.0 mg/L P) and high concentrations of hypolimnetic P were confined to ~ 0.5 m above the sediment-water interface (Fig. 10). As discussed below, mixing of this hypolimnetic P into the surface waters during epilimnetic expansion and fall turnover coincided with the development of an algal bloom that exceeded 60 µg/L chlorophyll, suggesting uptake of this P for growth (see Fig. 10 and 12).

Surface total P concentrations were relatively low (< 0.030 mg/L) between May and early July 2020 (Fig. 11). However, concentrations increased linearly between July and September to a peak of 0.074 mg/L. This surface total P peak coincided with peak chlorophyll concentrations, reflecting incorporation of P derived from the hypolimnion into algal biomass (Fig. 12). The surface total P concentration declined in late September through early October in conjunction with a decline in chlorophyll concentration (Fig. 11 and 12).

Similar to total P, surface chlorophyll concentrations were very low until early July (Fig. 12). Concentrations increased steadily between July and early August to a peak that exceeded 60 µg/L (Fig. 12). The chlorophyll maximum was short-lived, and concentrations declined to < 25 µg/L in late September-early October. The typical seasonal chlorophyll pattern in years prior to alum treatment saw a substantial increase in concentration during Fall turnover due to entrainment of hypolimnetic SRP and uptake by cyanobacteria (James et al. 2015). For instance, in 2010 chlorophyll increased from ~ 22 µg/L in mid-July to a maximum ~ 110 µg/L in early October (Fig. 12). Unlike Fall patterns in 2017 through 2020, chlorophyll concentrations remained high and maximal for extended periods (i.e., September through early November) during Fall turnover as in 2010.

Secchi transparency was high during the period of low chlorophyll concentrations in May-early July then declined steadily to ~ 1 m in association with the chlorophyll peak in early September (Fig. 13). Prior to alum treatment, as in 2010, Secchi transparency was often unusually high in June, exceeding 2 to 3 m (James 2014, 2015). Transparency declined to a minimum (< 1.0 m) during periods of extended cyanobacteria blooms driven by Fall turnover and hypolimnetic SRP entrainment (Fig. 13, 2010). Secchi transparency exhibited a significant inverse pattern to that of chlorophyll, indicating that light extinction was due to algae versus inorganic turbidity (Fig. 14).

A comparison of mean summer (July-early October) limnological response variables before alum treatment (i.e., 2010) versus 2020 is shown in Figure 14 and Table 2. Mean bottom total P and SRP concentrations increased in 2020 (Fig. 15), but were still ~ 65% and 72% lower,

Table 2. Summary of changes in lake water quality and sediment variables after the initial alum treatment in June 2017. Overall goals after completion of the treatment schedule (Table 4) are shown in the last column. ND = no data at the time of report production.

Variable			2010	2017	2018	2019	2020	Percent improvement over 2010 means				Goal after internal P loading
								2017	2018	2019	2020	
Lake	Mean (Jul-Oct)	Mean surface TP (mg/L)	0.074	0.051	0.058	0.035	0.050	31% reduction	22% reduction	53% reduction	34% reduction	< 0.040
		Mean bottom TP (mg/L)	0.583	0.088	0.246	0.082	0.203	85% reduction	58% reduction	86% reduction	65% reduction	< 0.050
		Mean bottom SRP (mg/L)	0.467	0.038	0.199	0.02	0.130	92% reduction	57% reduction	96% reduction	72% reduction	< 0.050
		Mean chlorophyll (ug/L)	47.63	25.17	19.08	24.31	27.88	47% reduction	60% reduction	49% reduction	41% reduction	< 15
		Mean Secchi transparency (ft)	4.27	6.28	5.41	6.81	5.43	46% increase	27% increase	59% reduction	27% reduction	12.1
	Early Fall peak (i.e. late August-early October)	Surface TP (mg/L)	0.130	0.081	0.115	0.042	0.074	38% reduction	11% reduction	68% reduction	43% reduction	NA
		Bottom TP (mg/L)	1.216	0.13	0.543	0.206	0.510	89% reduction	55% reduction	83% reduction	58% reduction	NA
		Bottom SRP (mg/L)	1.092	0.068	0.468	0.092	0.442	94% reduction	57% reduction	92% redcution	60% redcution	NA
		Chlorophyll (ug/L)	109.6	42.95	27.63	42.00	64.89	61% reduction	75% reduction	62% reduction	41% reduction	NA
		Secchi transparency (ft)	2.66	3.61	3.63	3.94	3.12	36% increase	37% increase	48% reduction	17% reduction	NA
Sediment[1]		Net internal P loading (kg/summer)	3,723	1,150	1,062	-77	1,351	69% reduction	71% reduction	100% reduction	64% reduction	< 400
		Net internal P loading (mg/m^2 d)	8.8	3.2	2.8	-0.5	2.8	64% reduction	66% reduction	100% reduction	68% reduction	< 1.5
		Sediment diffusive P flux (mg/m^2 d)	15.01	11.83	8.34	1.26	4.66	21% reduction	29% reduction	85% reduction	69% reduction	< 1.5
		Redox-P (mg/g)	0.457	0.298	0.307	0.238	0.415	35% reduction	33% reduction	48% reduction	9% reduction	< 0.100
		Al-bound P (mg/g)	0.097	0.170	0.331	0.216	0.342	75% increase	241% increase	123% increase	253% increase	NA

[1]Stations 2, 8, 13, 18, and 24

respectively, compared to pretreatment 2010 means (Table 2). Mean summer surface total P also increased to 0.050 mg/L, exceeding the mean target concentration of 0.040 mg/L (Table 2). Mean chlorophyll was higher at 28 μg/L in 2020 but 41% lower than the pretreatment mean. Finally, mean Secchi transparency declined from 6.8 ft in 2019 to 5.4 ft in 2020 (Fig. 15 and Table 2). Overall, these patterns echoed the relationship between elevated internal P loading during the summer of 2020, mixing and transfer of P to the surface, and algal uptake for growth in the late summer to early fall. Although limnological response variables were still improved post-treatment, as discussed below P binding within the Al floc was again overwhelmed by diffusive P flux from sediment.

Unlike the Al treatment year of 2019, Cedar Lake P mass exhibited seasonal increases in 2020 (Fig. 16). Peak lake P mass in 2020 was double at 2,014 kg versus to 2019 but still lower compared to a maximum of > 4,000 kg in 2010. As indicated in James (2014, 2015), summer P mass increases were due almost entirely to internal P loading from anoxic sediment prior to alum treatment. Net internal P loading was substantial in 2010 at 3,723 kg (Table 3). While it was negligible in 2019 as a result of the second alum treatment, net internal P loading increased in 2020 to 12 kg/d or 2.8 mg/m^2 d suggesting P binding inefficiency within the Al floc (Table 3). Still, the 2020 net internal P loading rate represented a > 60% reduction over the rate estimated for the summer of 2010 (Table 2).

Table 3. Summer net internal phosphorus loading ($P_{net\ int\ load}$) estimates (bold font) for Cedar Lake in 2010 (pretreatment) and 2017-19 (post-treatment).

Summer	Period	$P_{tributary}$	$P_{discharge}$	$P_{retention}$	$P_{lake\ storage}$	$P_{net\ int\ load}$		
	(d)	(kg)	(kg)	(kg)	(kg)	(kg)	(kg/d)	(mg/m^2 d)
2010	97	445	238	207	3,931	**3,723**	**38**	**8.8**
2017	83	349	212	137	1,287	**1,150**	**14**	**3.2**
2018	87	279	122	157	1,227	**1,062**	**12**	**3.0**
2019	85	346	141	205	28	**-77**	**-1**	**0**
2020	112	456	369	87	1,434	**1,351**	**12**	**2.8**

The pattern of seasonal P mass increase in the epilimnion versus the hypolimnion remained improved in 2020 versus 2010 (Fig. 17). In 2010 (before Al application), the anoxic hypolimnion accounted for most of the seasonal P mass increase (Fig. 17). By comparison, hypolimnetic P mass accumulation was lower in 2020, indicating some suppression of net internal P loading from anoxic sediment (Fig. 17).

Changes in sediment chemistry and anaerobic diffusive phosphorus flux

Laboratory-derived anaerobic diffusive P fluxes increased in 2020 at both the central WQ2 station and stations located along the north-south transect one year after the 2019 Al application (Fig. 18). Although lower than the pretreatment rate of 8.8 mg/m^2 d by 69%, the mean anaerobic diffusive P flux along all transect stations was still moderately high at 4.7 mg/m^2 d in 2020 (Table 2). This increase corroborated with similar patterns of increase in lake P mass accumulation (Fig. 19) and declines in limnological response variables in 2020 (Table 2).

Similar to patterns at the centrally located WQ 2 (Fig. 18), anaerobic diffusive P flux declined substantially at all stations located along the North-to-South transect in conjunction with the second Al application in 2019 (Fig. 20). Although still low relative to pretreatment sediment P fluxes, rates unfortunately rebounded at all stations in 2020. Flux increases in 2020 were greatest at the northern-most station 2, the centrally located station 13, and station 18, located in the southern portion of the deep basin at 5 mg/m^2 d or greater (Fig. 20).

Vertically in the sediment column at station WQ 2 concentrations of redox-bound P were still lower in the upper 5 cm sediment layer in 2020 relative to June 2017 (Fig. 21). Aluminum-bound P concentrations were elevated in the upper 6 cm of sediment, reflecting binding of P by the Al floc (Fig. 21). Total Al concentrations were highest in the upper 4-cm sediment layer. A secondary lower Al concentration peak occurred at the 6-7-cm depth (Fig. 21). Total Al in the upper 7-cm sediment layer was 49.7 g/m^2. Assuming all the Al and aluminum-bound P in the upper 7-cm sediment layer was added from the 2 alum treatments (i.e., no background natural Al), the Al:Al-bound P ratio was ~ 43:1 at WQ 2. The future target ratio should be < 20:1.

Variations in redox-P and aluminum-bound P in the upper 5-cm sediment layer at individual stations located along the north-south transect (i.e., stations 2, 8, 13, 18, and 24, Fig. 1) are shown in Fig. 20. Overall, aluminum-bound P exhibited a trend of increasing concentration at all stations as a result of the two Al treatments, suggesting P binding onto the alum floc. Aluminum-bound P concentrations were generally greatest in 2020 at all stations except station 2 (Fig. 20). In addition, highest aluminum-bound P concentrations occurred at station 8, 13, and 18, located within the 25-ft depth contour. This area also received the highest Al doses in 2017 and 2019. In contrast, redox-P concentration tended to decline in 2019, after the second Al application, but then rebounded in 2020 to higher concentrations. This pattern suggested that P from deeper sediment layers could be diffusing upward to the sediment surface with limited binding onto the Al floc layer, indicating the Al floc could be polymerizing and forming crystals which tie up bindings sites that would otherwise be available for P. Elevated redox-P also coincided with higher diffusive P flux in 2020, further suggesting the Al floc was perhaps losing binding sites for P due to crystallization and was now becoming overwhelmed with P diffusing upward from deeper sediment layers.

Changes in total Al in the upper 5-cm sediment layer after the two partial Al applications suggested uneven distribution of the Al floc after treatment (Fig. 22). For instance, total Al concentrations increased at station 2, 18, and 24 in 2017 (after the first Al application) and 2020 (after the 2019 Al application) relative to pretreatment levels. However, concentrations remained similar or declined in 2020 compared to pretreatment levels at stations 8 and 13, located in the central deep basin. Assuming all the total Al in the upper 5-cm sediment layer was from alum application only (i.e., no background natural Al), area-based concentrations were lower than the theoretical target at all but station 24 (Fig. 23). These trends may not be statistically significant; however, the overall patterns may be attributed to a couple of factors. First, some of the alum may have mixed downward below the 5-cm sediment depth and was, thus, not measured and accounted for in the calculation. Thus, lower Al recovery (i.e., the added alum) may be attributed to sectioning only the upper 5-cm sediment layer. Second, the Al floc may have moved or become redistributed during or after application by wind activity and water currents. Al floc movement during settling is not uncommon and has been reported to occur in other alum treatments (Huser 2012, Egemose et al. 2013, James and Bischoff 2019). Al floc redistribution in Cedar Lake may not be surprising given the large lake surface area and long fetch along the North-South wind rose.

Recommendations

It is recommended the Lake District strongly consider applying all the 3rd scheduled Al application to the > 25-ft depth contour in 2021. While the first two Al applications (2017 and 2019) have been temporarily effective in suppressing internal P loading during the year of treatment, diffusive P flux from sediment has overwhelmed the Al floc layer binding capacity in the two nontreatment years (2018 and 2020). This pattern has resulted in some hypolimnetic P accumulation (albeit much lower than in 2010), P mixing into the surface waters during the onset of fall turnover, and stimulation of fall algal blooms, particularly in 2020. Obviously, the current Al floc concentration from the 2 partial dose treatments is not yet high enough to completely bind the internal P load from sediment. Application of a higher partial Al dose to depths > 25 ft in 2021 would lead to longer control internal P loading and suppress algal bloom formation until the final partial dose is applied in ~ 2025.

The current application plan (Fig. 24) calls for two alum treatment zones with partial dose applications of ~ 20 g/m^2 within the 20-25 ft depth contour and ~ 26 g/m^2 for depths > 25 ft (i.e., third partial alum treatment, Fig. 22). As 2020, most of the hypolimnetic anoxia and P accumulation was confined to depths > 7.5 m or 25 ft, arguing for concentrating the third partial dose to only this area (Fig. 25). Without increasing costs, Al application to depths > 25 ft only in 2021 would result in an Al concentration of 50 g/m^2 versus 26 g/m^2, leading to a theoretical total Al concentration of > 90 g/m^2 in this area after the third treatment. The success of this 2021 application in maintaining target limnological goals will be assessed (monitoring and adaptive management) and information gleaned will be used to adjust the application timing, treatment area, and Al dosage of the fourth and fifth treatments.

References

APHA (American Public Health Association). 2011. Standard Methods for the Examination of Water and Wastewater. 22th ed. American Public Health Association, American Water Works Association, Water Environment Federation.

Avnimelech Y, Ritvo G, Meijer LE, Kochba M. 2001. Water content, organic carbon and dry bulk density in flooded sediments. Aquacult Eng 25:25-33.

de Vicente I, Huang P, Andersen FØ, Jensen HS. 2008. Phosphate adsorption by fresh and aged aluminum hydroxide. Consequences for lake restoration. Environ Sci Technol 42:6650-6655.

Håkanson L, Jansson M. 2002. Principles of lake sedimentology. The Blackburn Press, Caldwell, NJ USA.

Hjieltjes AH, Lijklema L. 1980. Fractionation of inorganic phosphorus in calcareous sediments. J Environ Qual 8: 130-132.

James WF. 2012. Limnological and aquatic macrophyte biomass characteristics in Half Moon Lake, Eau Claire, Wisconsin, 2012: Interim letter report. University of Wisconsin – Stout, Sustainability Sciences Institute – Discovery Center, Menomonie, WI.

James WF. 2014. Phosphorus budget and management strategies for Cedar Lake, WI. University of Wisconsin – Stout, Sustainability Sciences Institute – Discovery Center, Menomonie, WI.

James WF. 2017. Phosphorus binding dynamics in the aluminum floc layer of Half Moon Lake, Wisconsin. Lake Reserv Manage 33:130-142.

James WF, PW Sorge, PJ Garrison. 2015. Managing internal phosphorus loading in a weakly stratified eutrophic lake. Lake Reserv Manage 31:292-305.

Mortimer CH. 1971. Chemical exchanges between sediments and water in the Great Lakes – Speculations on probable regulatory mechanisms. Limnol Oceanogr 16:387-404.

Nürnberg GK. 1988. Prediction of phosphorus release rates from total and reductant-soluble phosphorus in anoxic lake sediments. Can J Fish Aquat Sci 45:453-462.

Nürnberg GK. 2009. Assessing internal phosphorus load – Problems to be solved. Lake Reserv Manage 25:419-432.

Pilgrim KM, Huser BJ, Brezonik PL. 2007. A method for comparative evaluation of whole-lake and inflow alum treatment. Wat Res. 41:1215-1224.

Psenner R, Puckso R. 1988. Phosphorus fractionation: Advantages and limits of the method for the study of sediment P origins and interactions. Arch Hydrobiol Biel Erg Limnol 30:43-59.

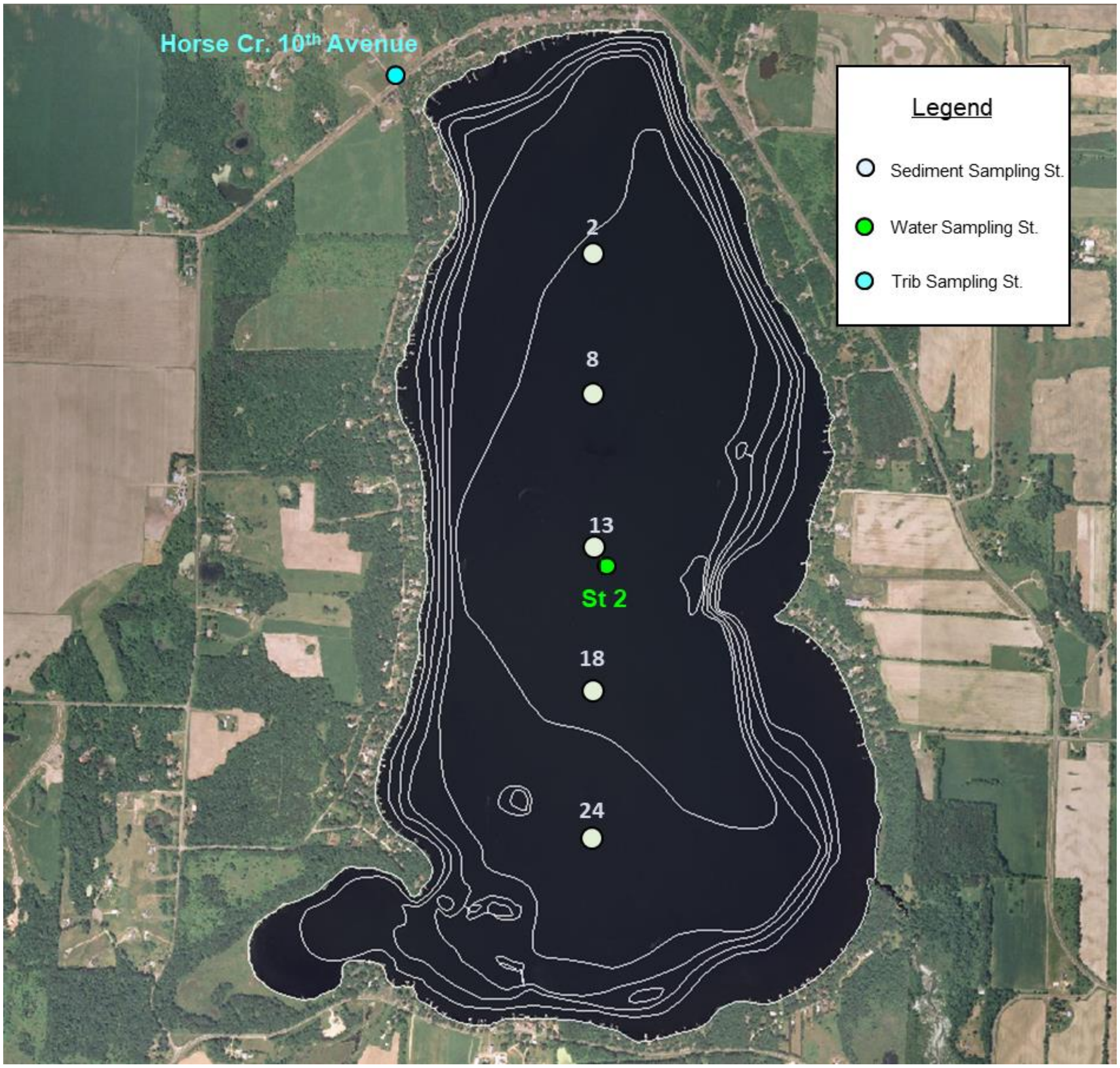

Figure 1. Sediment and water sampling stations.

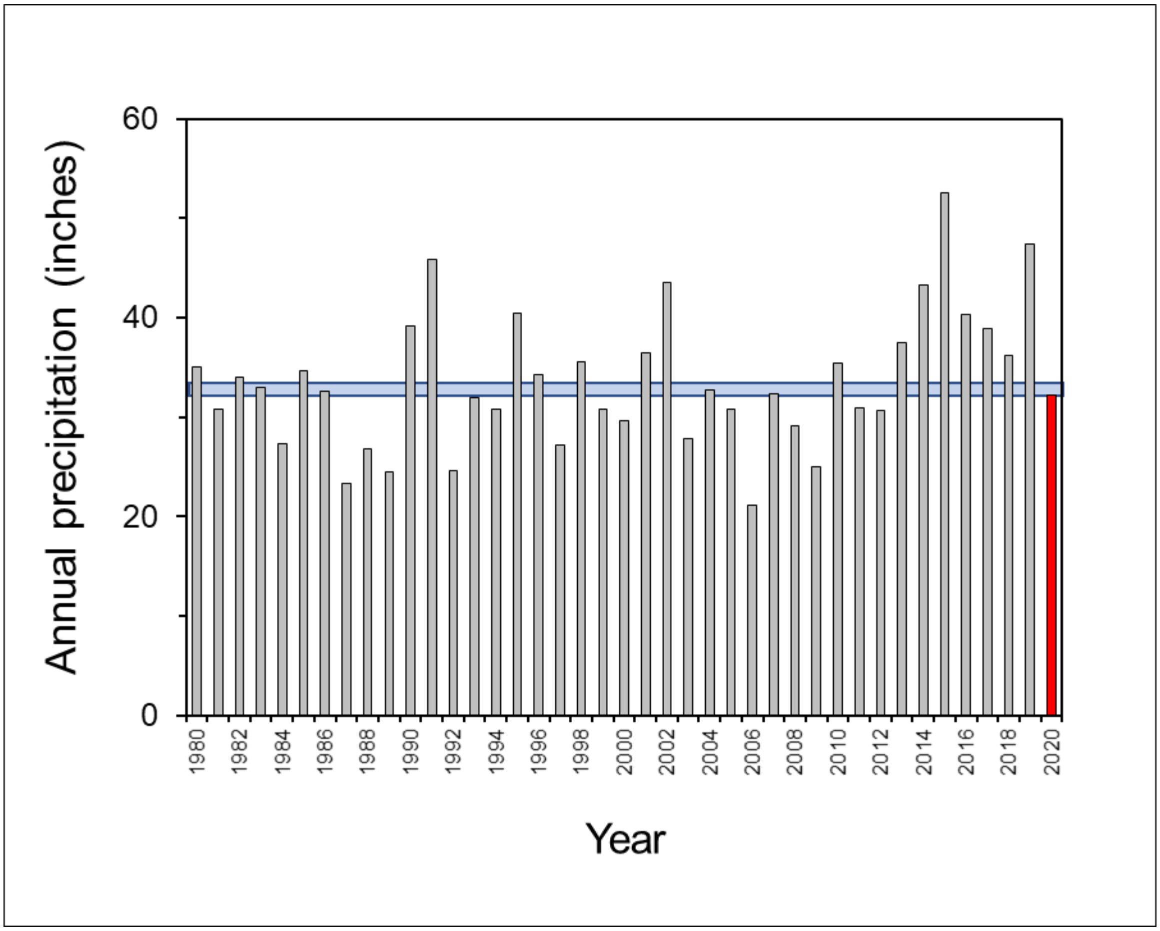

Figure 2. Variations in annual precipitation at Amery, WI. Blue horizontal line represents the average. The year 2020 is highlighted in red.

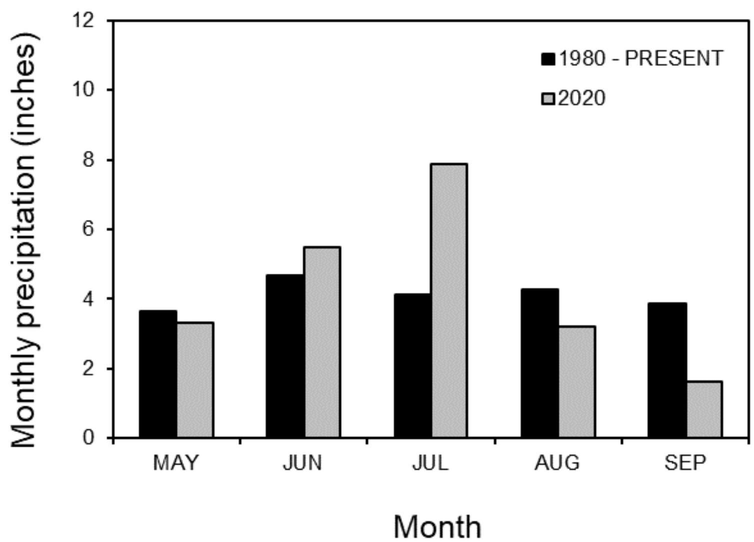

Figure 3. A comparison of average monthly precipitation.

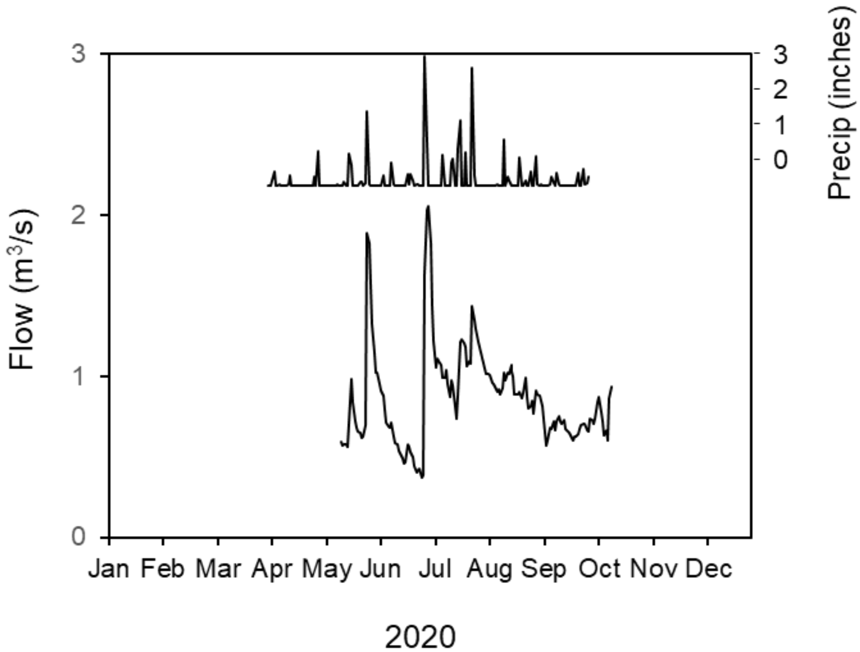

Figure 4. Seasonal variations in daily precipitation at Amery, WI, and flow for Horse Creek at 10^{th} Ave.

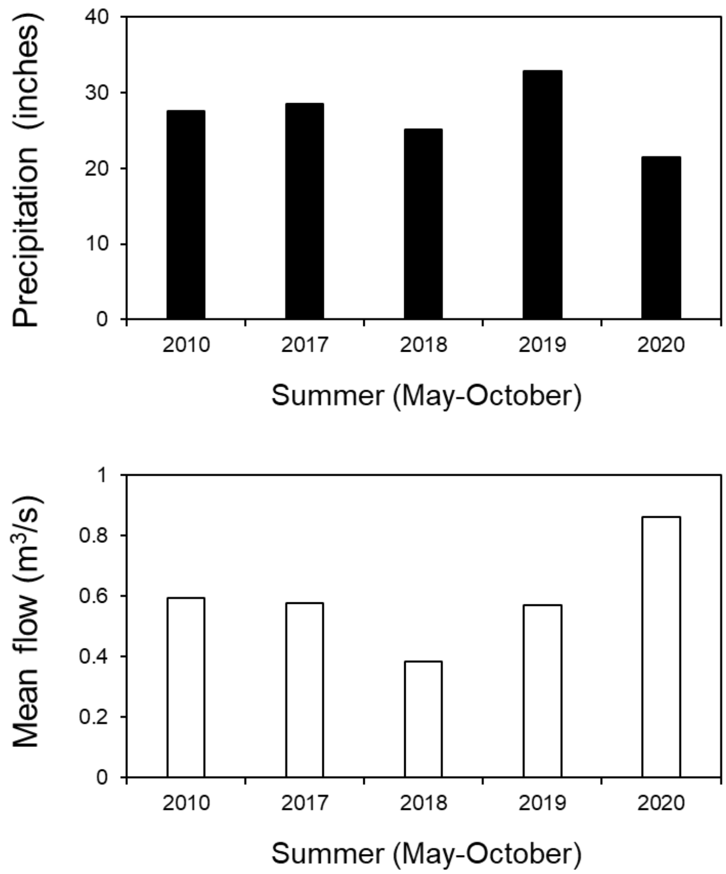

Figure 5. A comparison of summer (May-October) precipitation (upper panel) and mean Horse Creek flow (lower panel). The summer of 2010 was a pretreatment year. Alum was applied to the lake in late June 2017 and 2019.

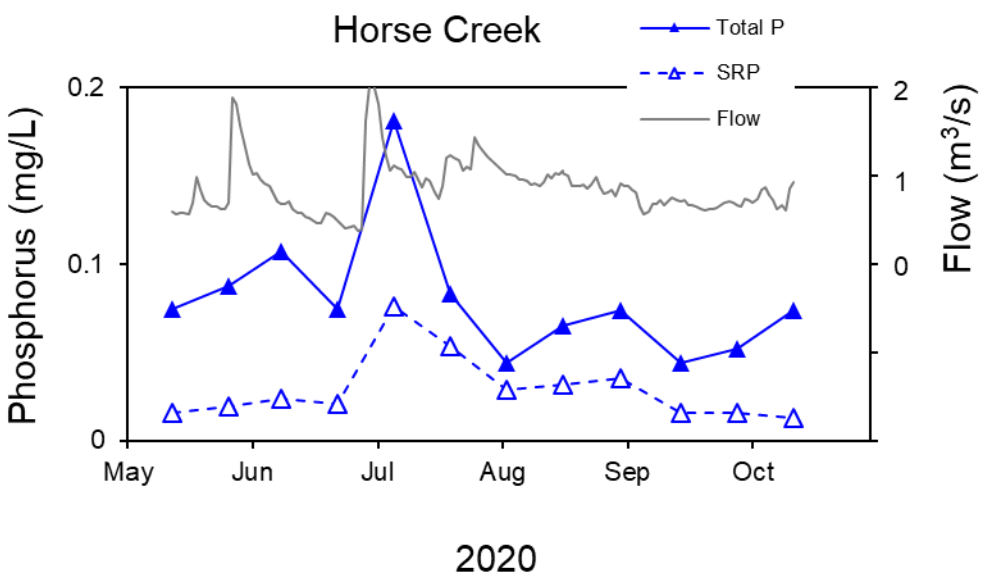

Figure 6. Seasonal variations in total phosphorus (P) and soluble reactive P (SRP) concentration at Horse Creek.

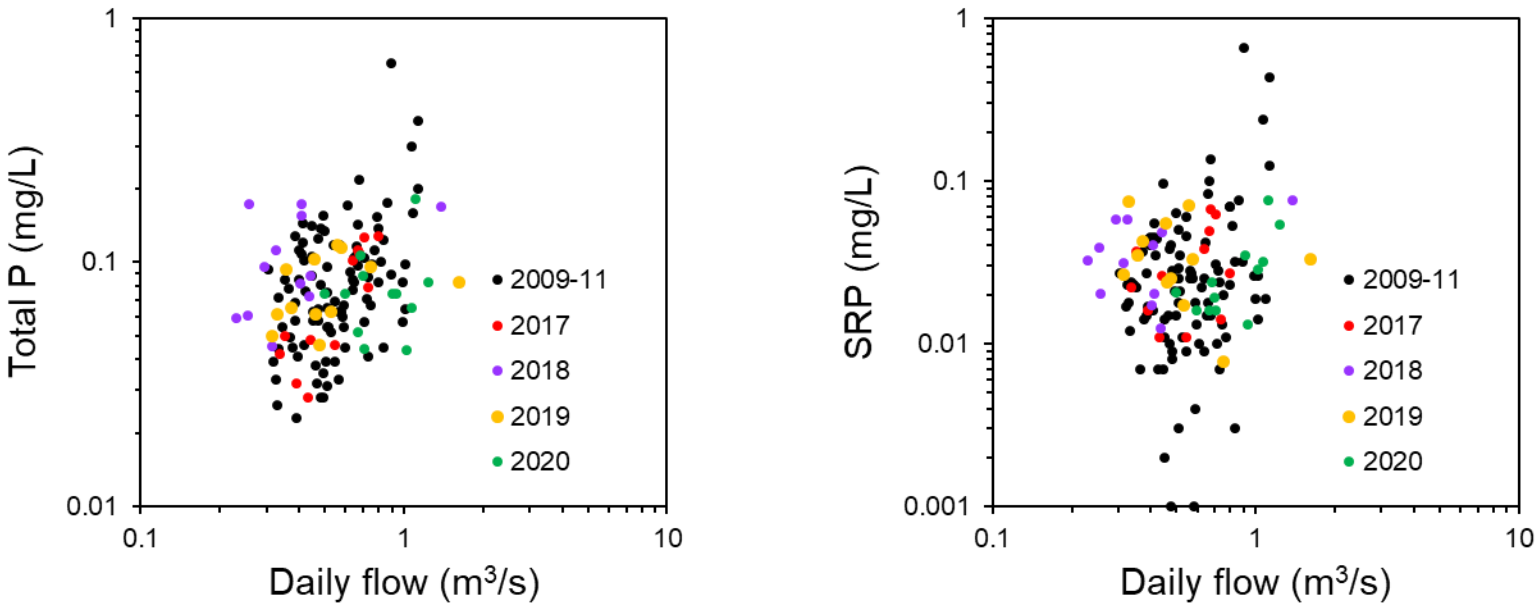

Figure 7. Phosphorus (P) concentration versus daily flow at Horse Creek.

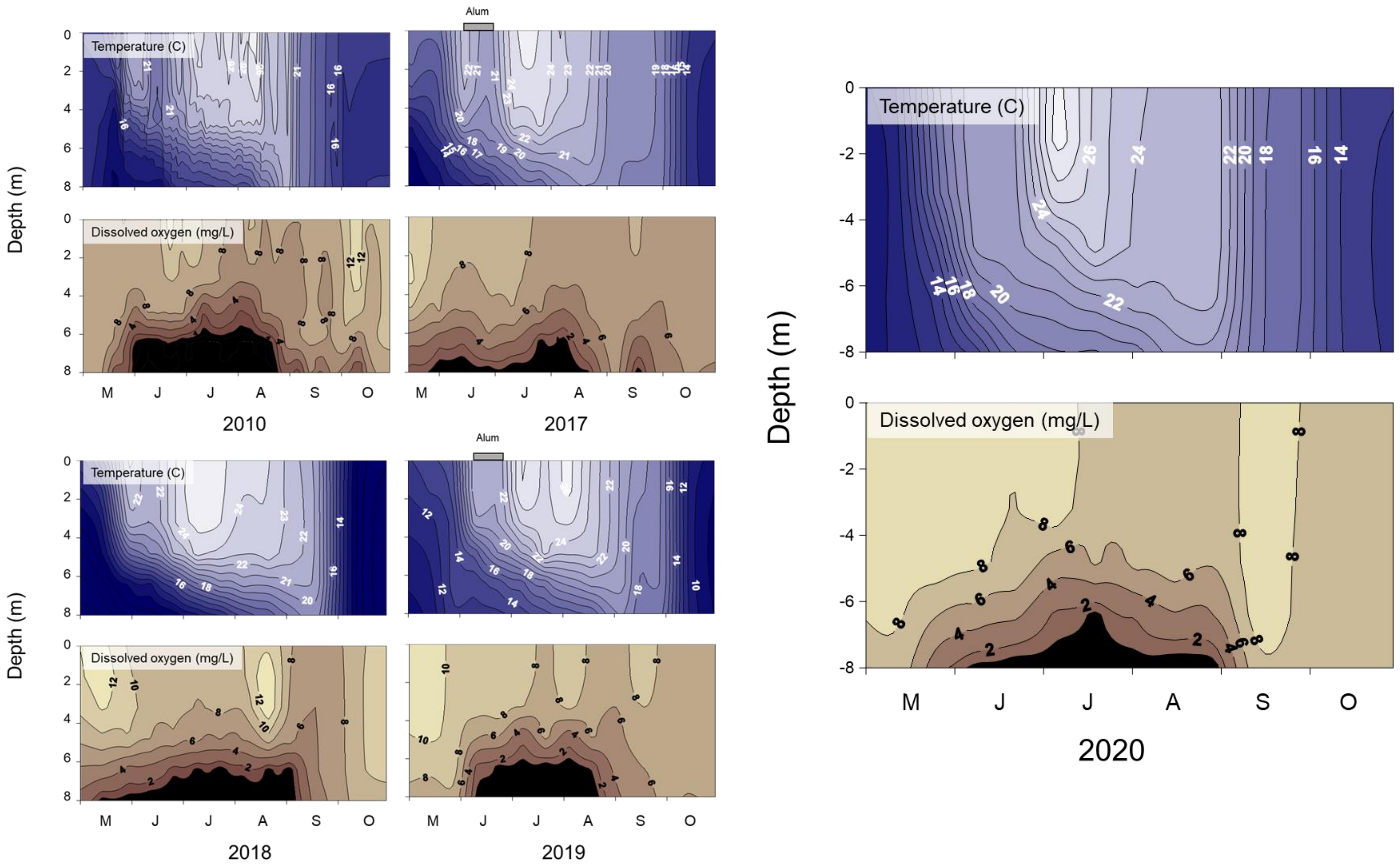

Figure 8. Seasonal and vertical variations in temperature (upper panels) and dissolved oxygen (lower panels) in 2010 (pre-treatment) and 2017-2020 (after alum treatment). Alum was applied in June 2017 and June 2019.

Figure 9. Seasonal variations in bottom (i.e., ~ 0.25 m above the sediment-water interface) total phosphorus (P), and bottom soluble reactive P (SRP) during a pretreatment year (2010) and the post-alum treatment years 2017-20. Alum was applied in June 2017 and June 2019.

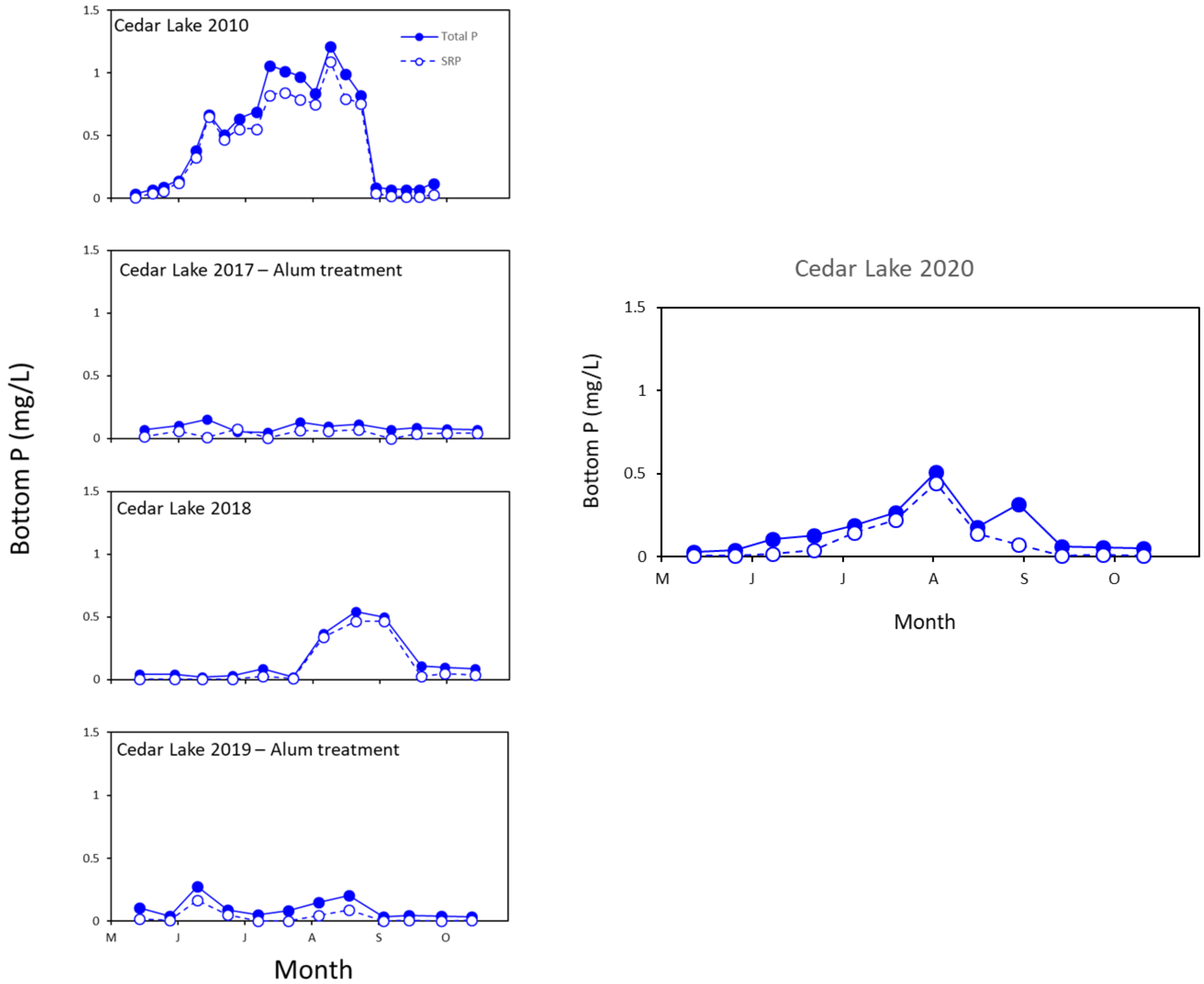

Figure 10. Seasonal and vertical variations in a) total phosphorus (P), b) soluble reactive P, and c) chlorophyll in 2010 (pretreatment) versus 2017-20 (post-treatment). Alum was applied in June 2017 and June 2019.

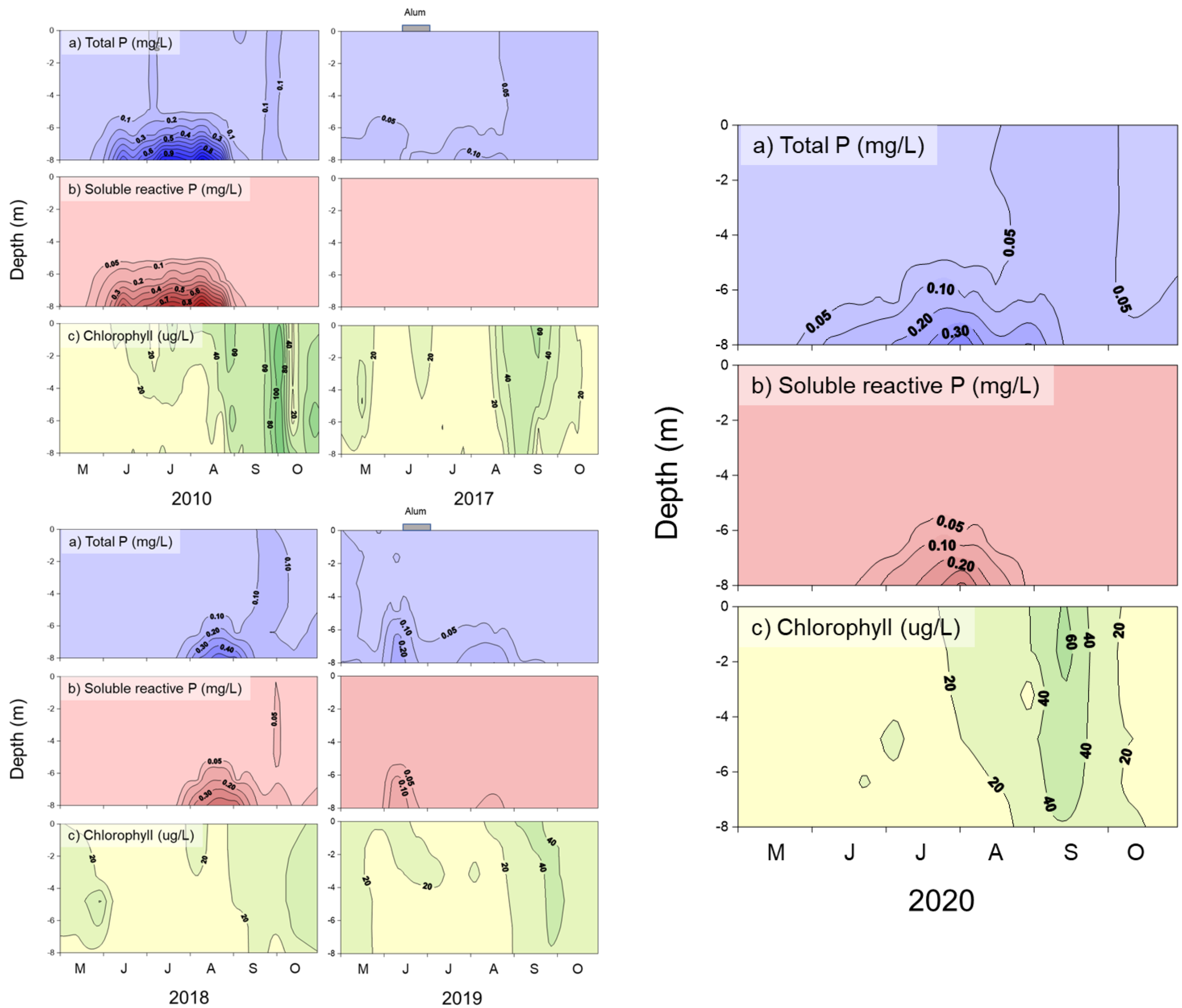

Figure 11. Seasonal variations in surface total phosphorus (P), during a pretreatment year (2010) and the post-alum treatment years 2017-20. Alum was applied in June 2017 and June 2019.

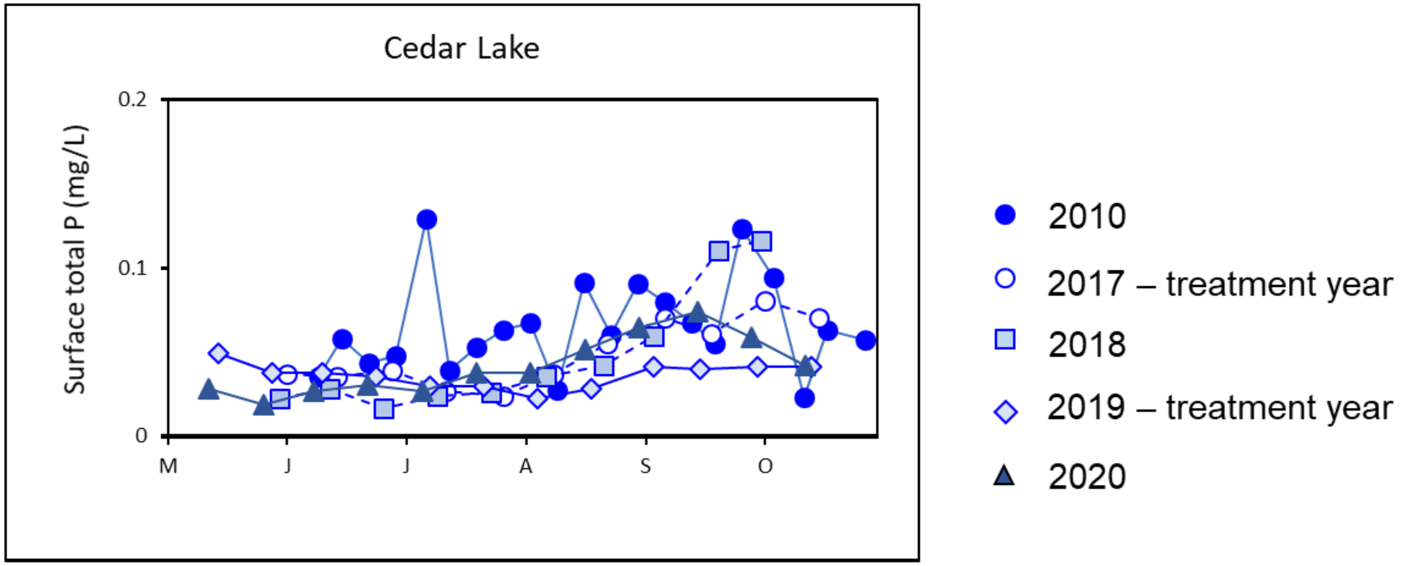

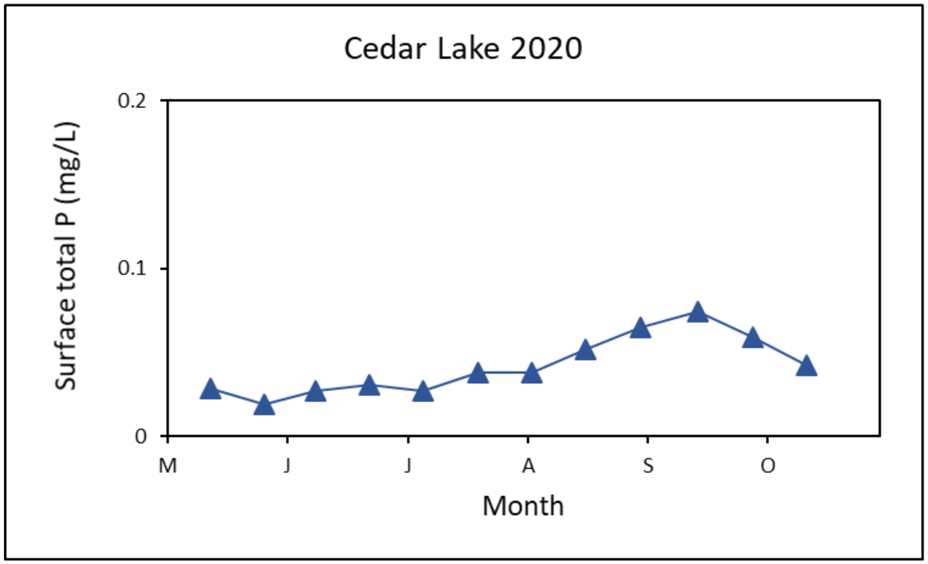

Figure 12. Seasonal variations in surface chlorophyll during a pretreatment year (2010) and the post-alum treatment years 2017-20. Alum was applied in June 2017 and June 2019.

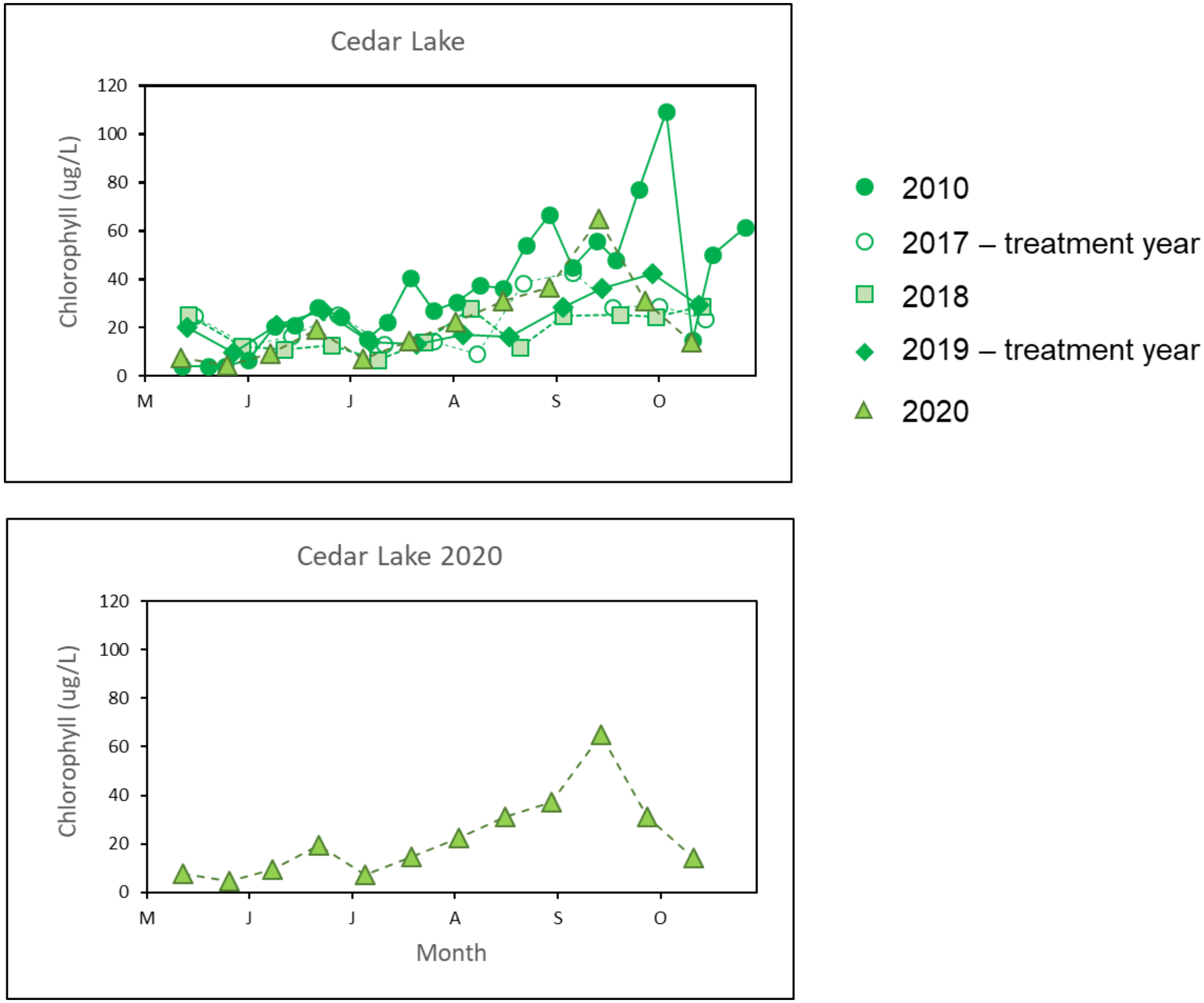

Figure 13. Seasonal variations in Secchi transparency during a pretreatment year (2010) and the post-alum treatment years 2017-20. Alum was applied in June 2017 and June 2019.

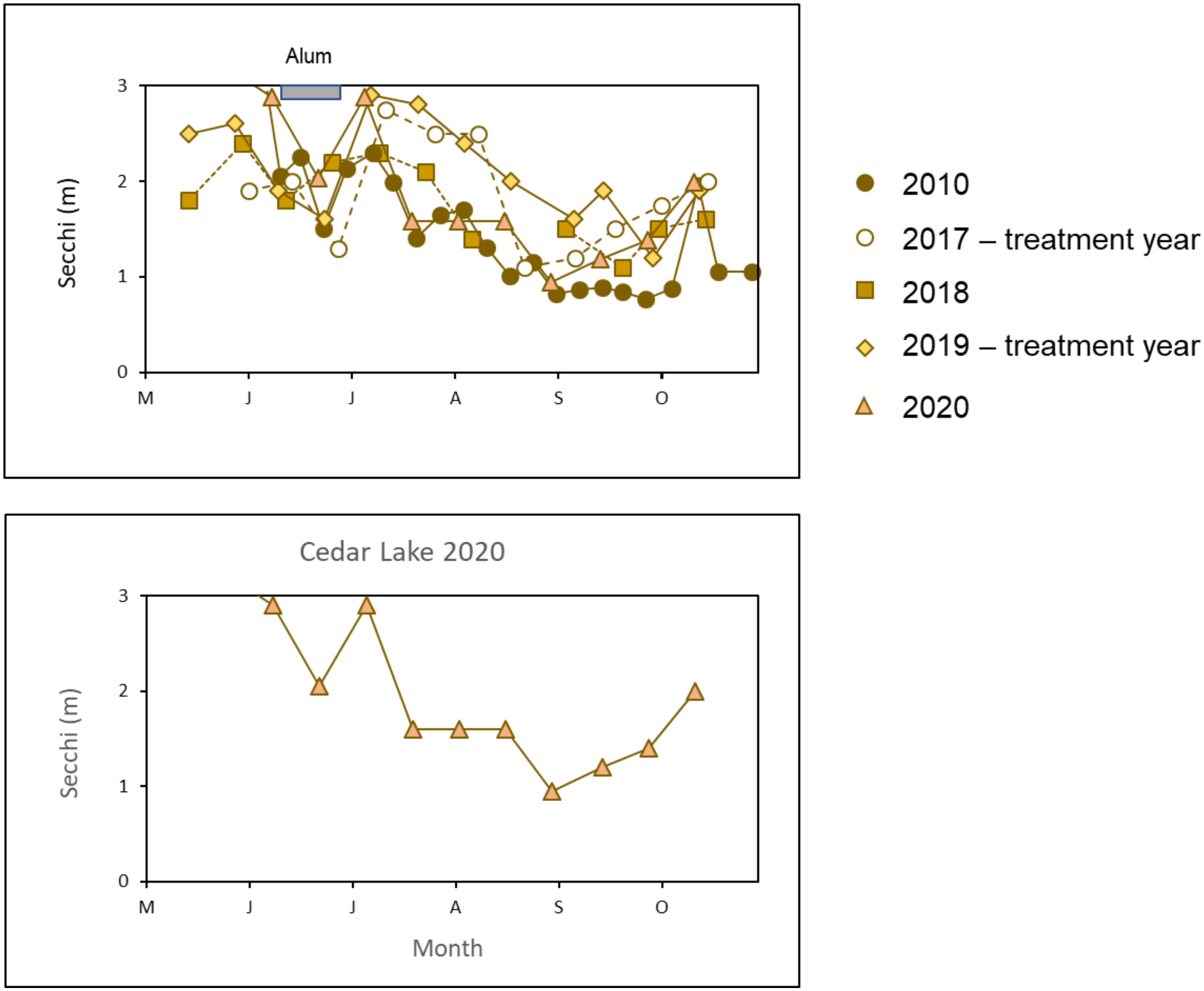

Figure 14. Relationships between Secchi transparency and chlorophyll (upper panel) and total phosphorus (P) versus chlorophyll (lower panel) during the summer 2017-2020.

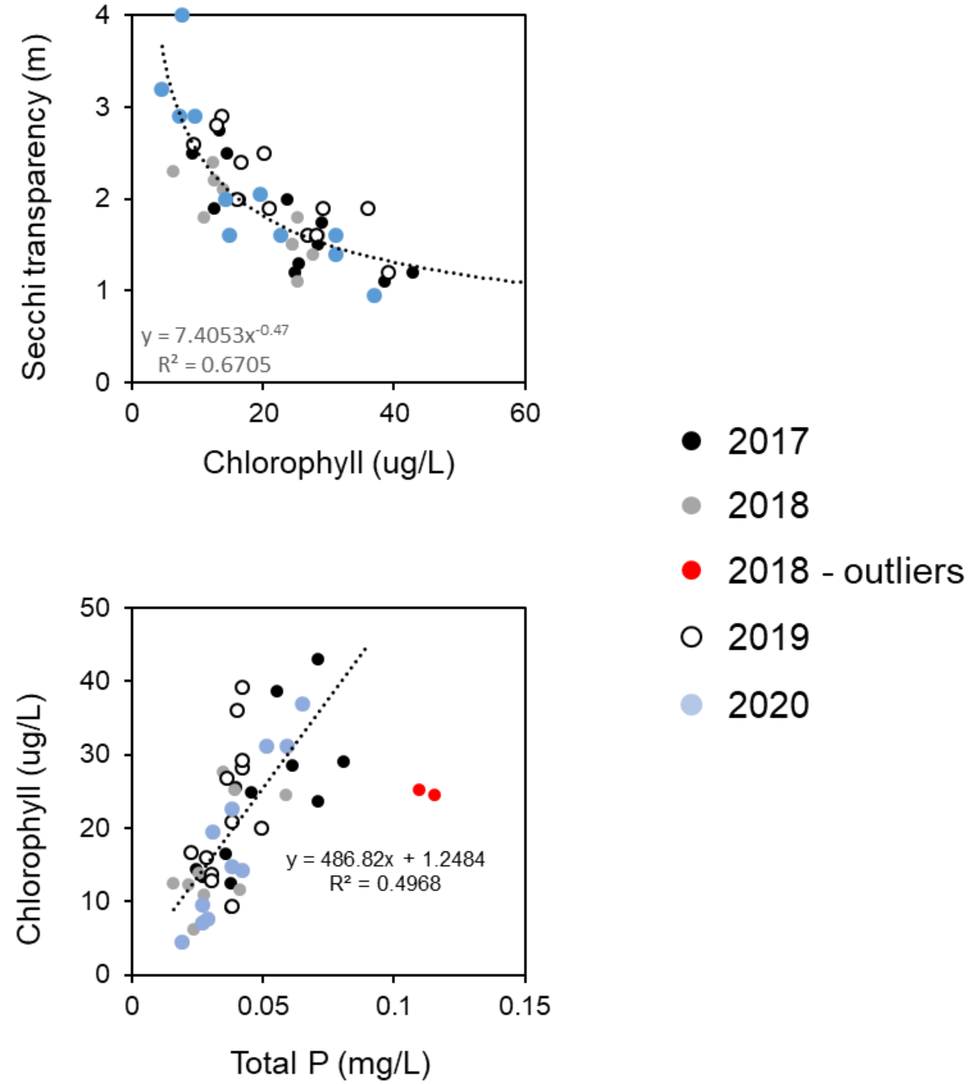

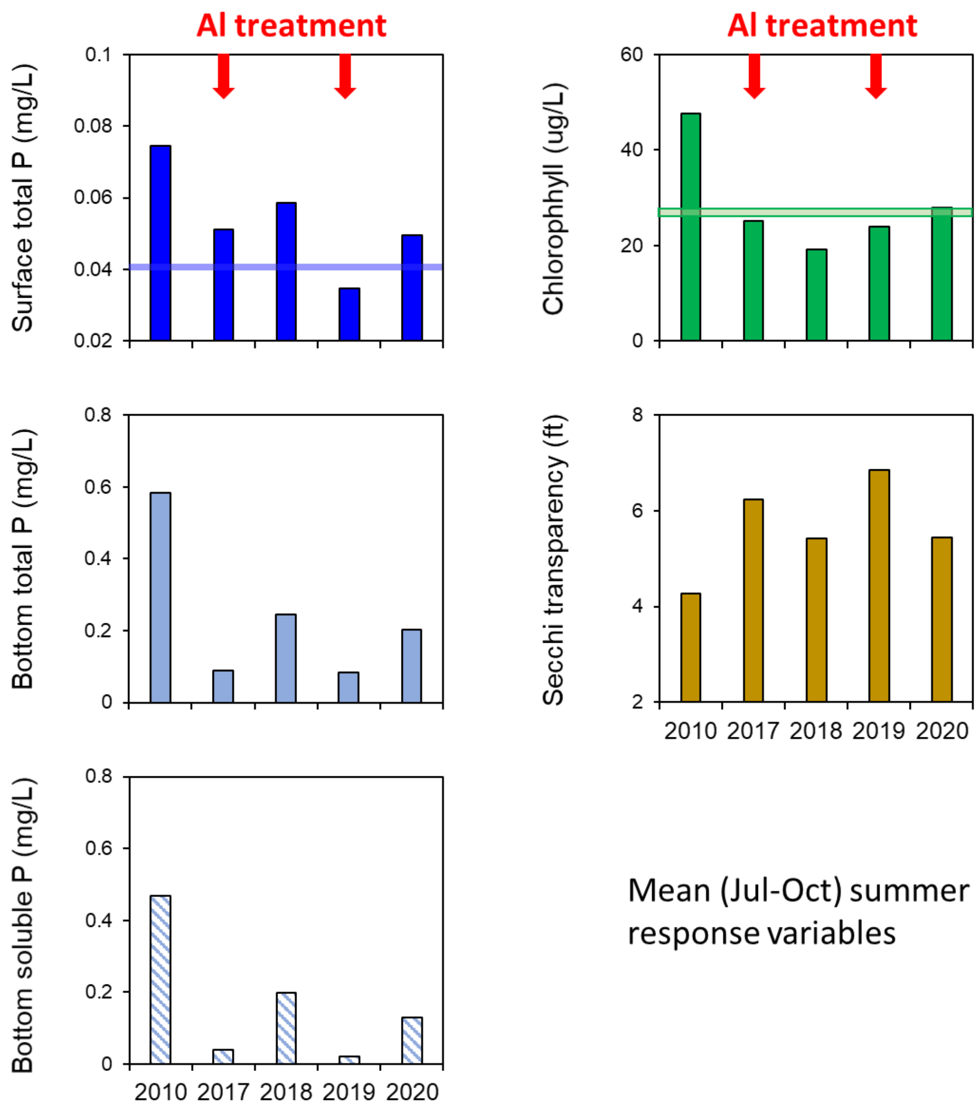

Figure 15. A comparison of mean summer (July-early October) summer concentrations of surface and bottom total phosphorus (P) and soluble reactive P (SRP), chlorophyll and Secchi transparency during a pretreatment year (2010) and the post-treatment years 2017-20. Alum was applied in June 2017 and June 2019.

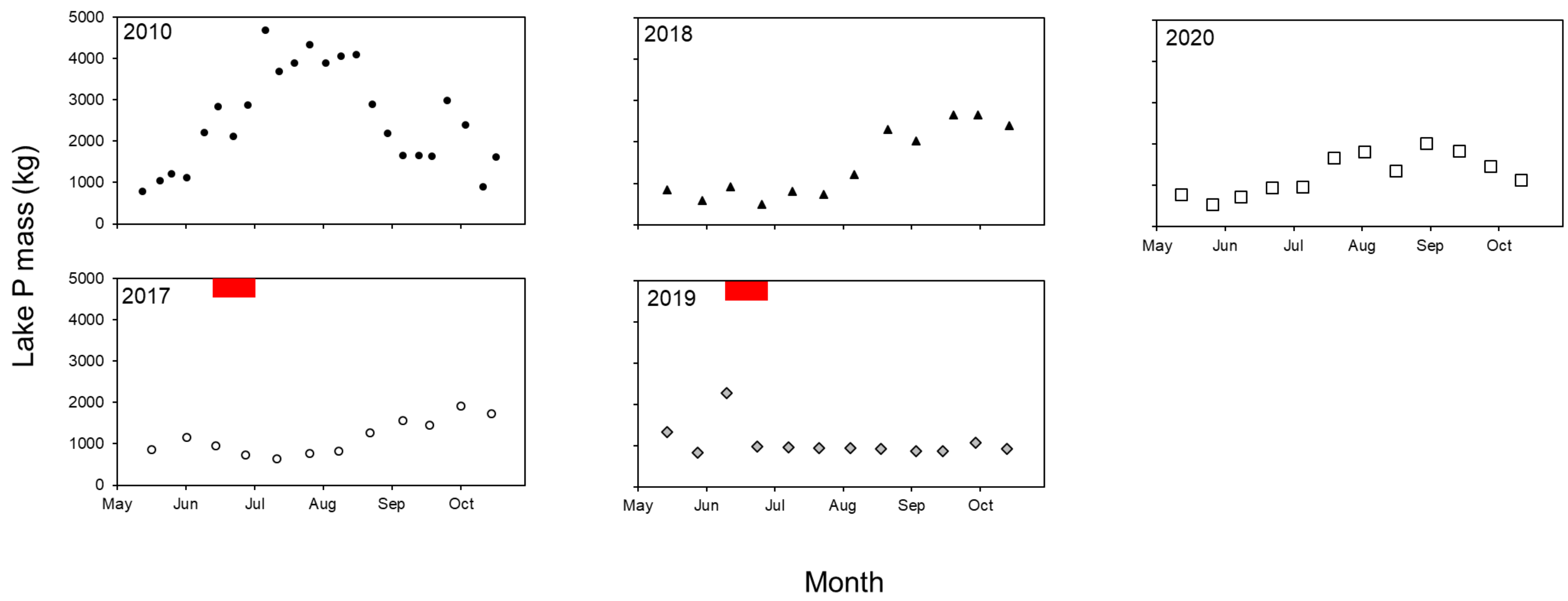

Figure 16. Seasonal variations in total phosphorus (P) mass during a pretreatment year (2010) and the post-treatment years 2017-20. Alum was applied in June 2017 and June 2019.

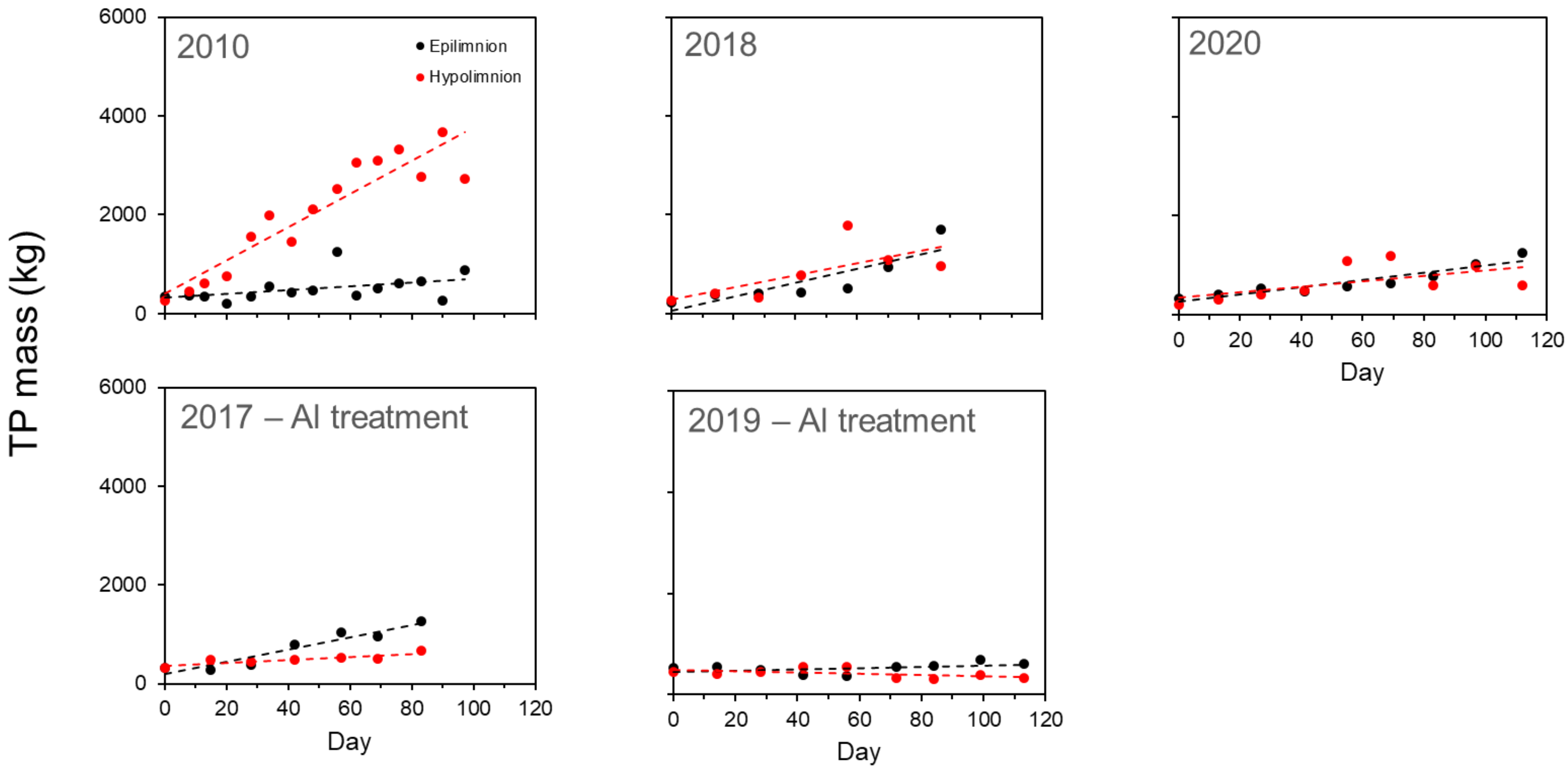

Figure 17. Seasonal variations in total phosphorus (P) mass in the epilimnion (i.e., 0-4 m) and hypolimnion (> 4 m) during a pretreatment year (2010) and the post-treatment years 2017-20. Alum was applied in June 2017 and June 2019.

Figure 18. Variations in anaerobic diffusive phosphorus (P) flux (mg/m^2 d) before (June 2010 and 2017) and after the first and second alum application. WQ-2 = the centrally-located water quality sampling station. Spatial = the means from stations 3, 8, 13, 18, and 24 (see Fig. 1)

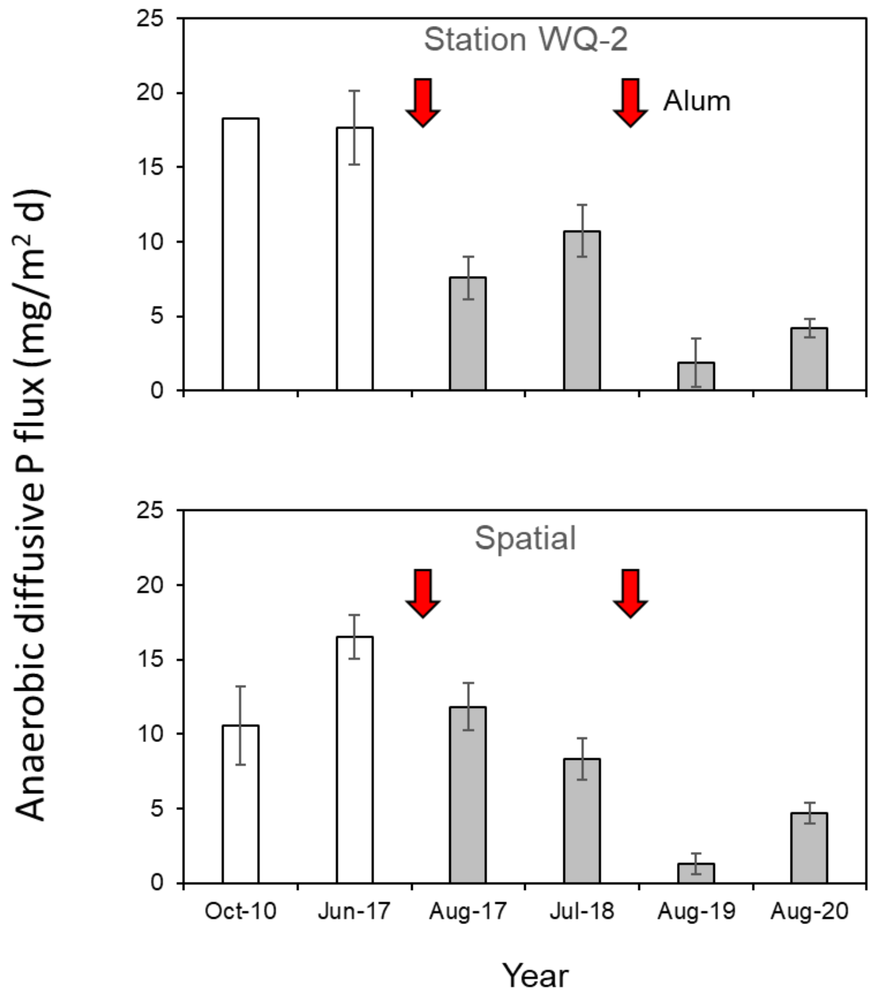

Figure 19. Variations lake phosphorus (P) mass accumulation before (June 2010 and 2017) and after the first and second alum application.

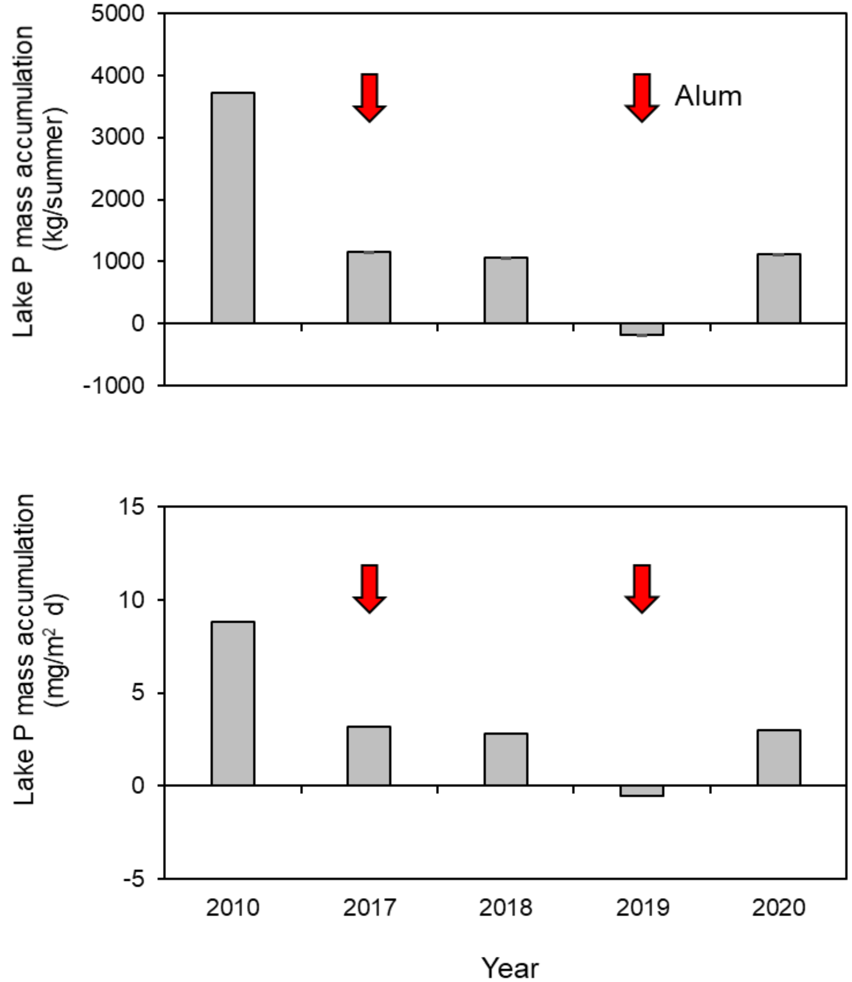

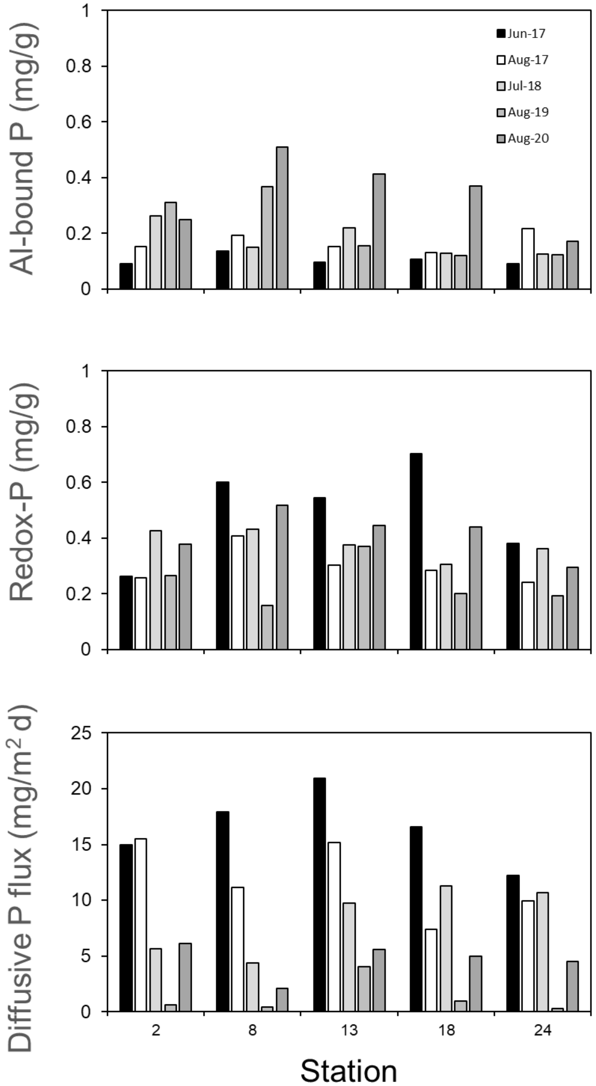

Figure 20. Variations in aluminum-bound phosphorus (Al-bound P) and redox-P in the upper 5-cm sediment layer, and laboratory-derived anaerobic diffusive P flux at various stations (please see Fig. 1). Partial alum treatments occurred in 2017 and 2019.

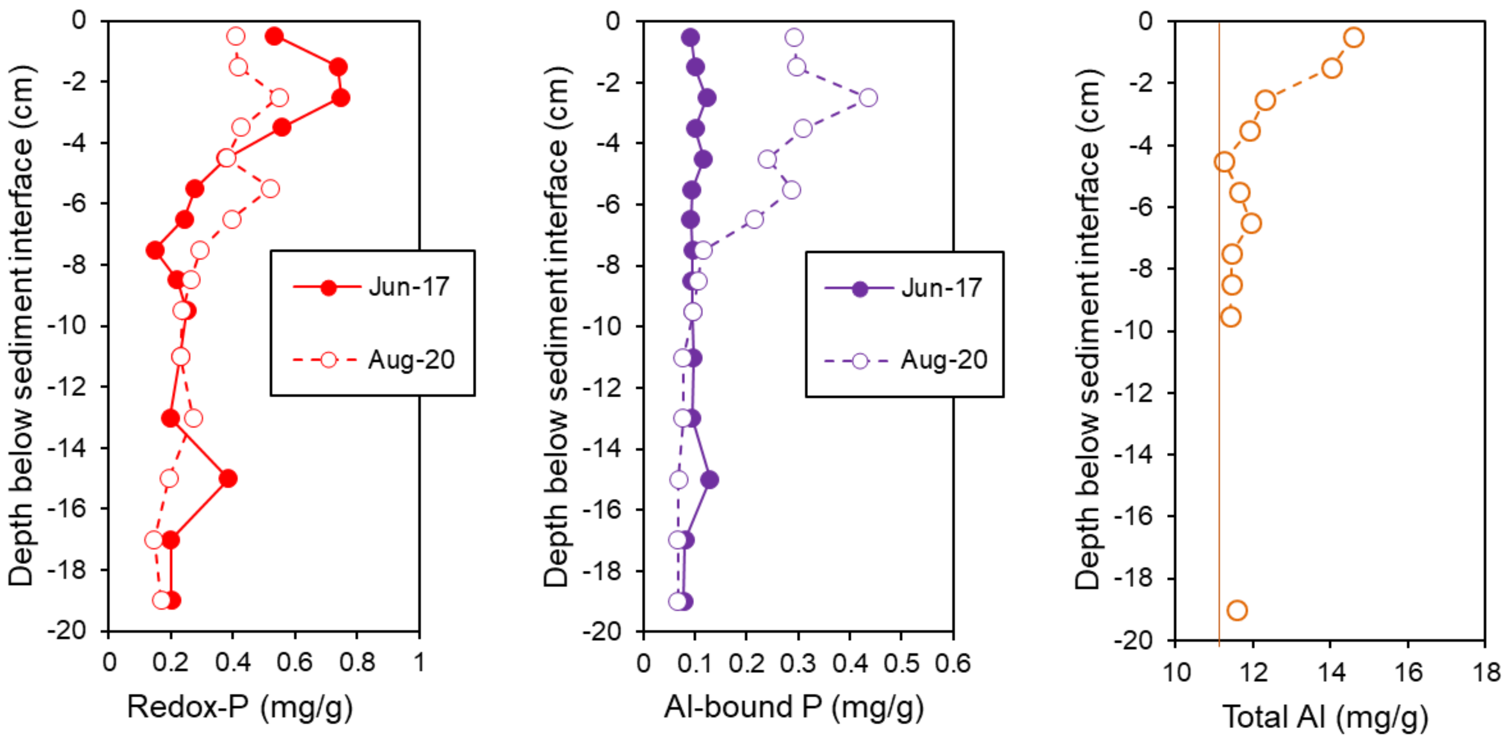

Figure 21. Vertical variations in sediment redox (i.e., the sum of the loosely-bound P and iron-bound P sediment fractions) phosphorus (P), aluminum (Al)-bound P, and total aluminum (Al) concentrations for a sediment core collected from station 2 (Figure 1) in June 2017 and August 2020. The sediment profile in June of 2017 represents pre-treatment conditions while August 2020 represents post-alum treatment conditions after two alum applications (2017 and 2019).

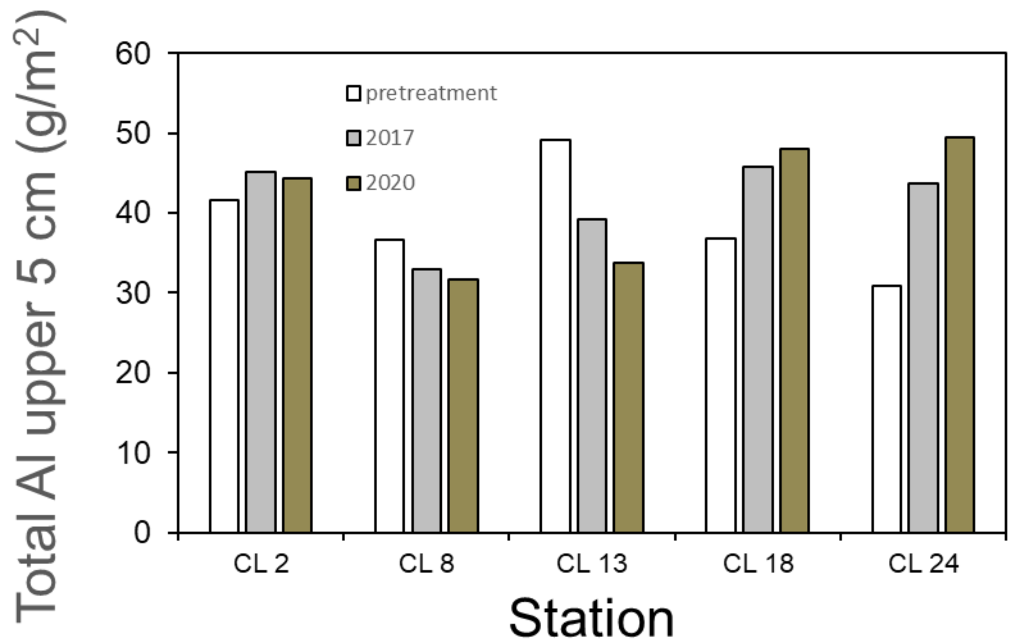

Figure 22. Variations in total aluminum (Al) in the upper 5-cm sediment layer at various stations (please see Fig. 1). Partial alum treatments occurred in 2017 and 2019.

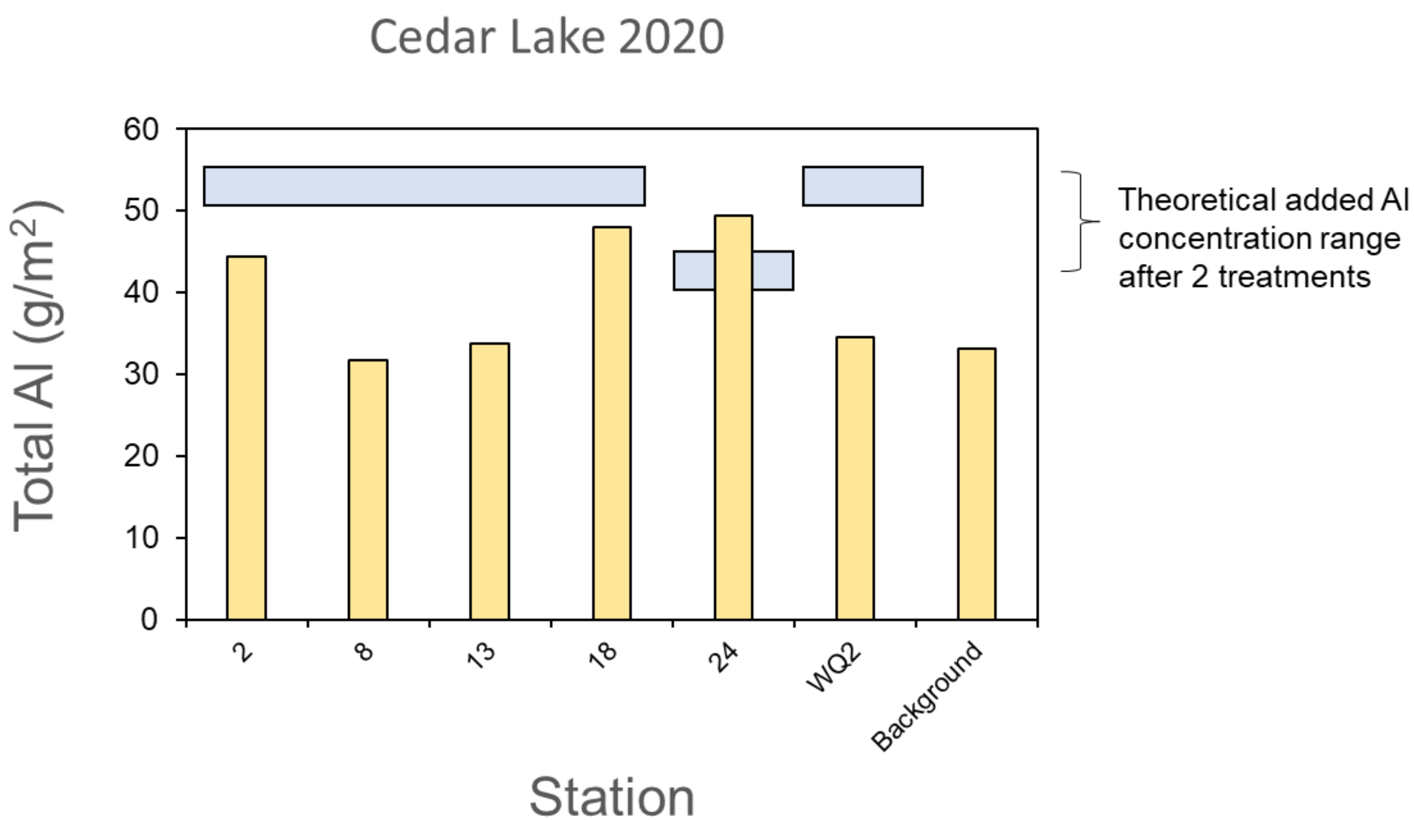

Figure 23. Total aluminum (Al) in the upper 5-cm sediment layer for various stations (please see Fig. 1) along the North-South transect in 2020.

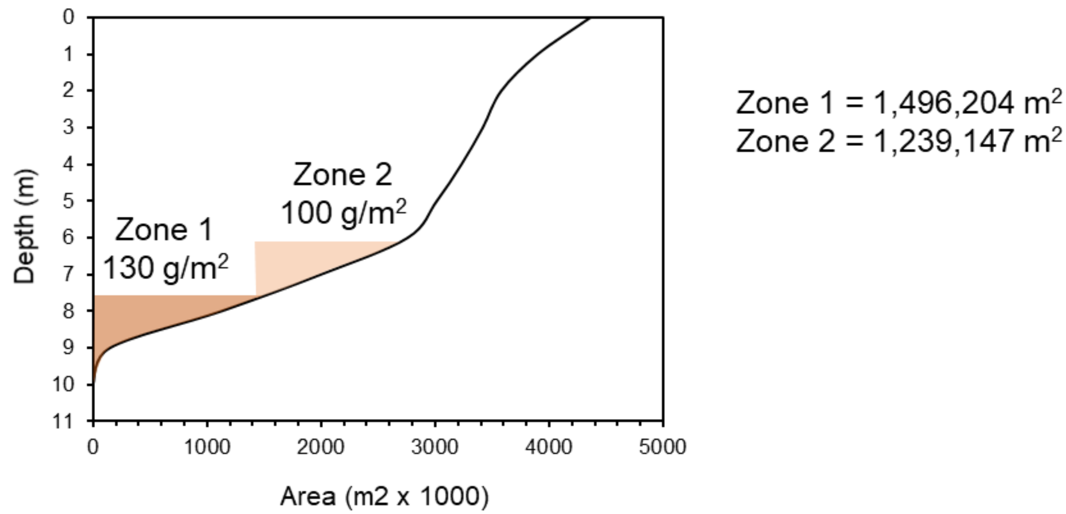

Figure 24. Lake area versus lake depth hypsography showing the location of the 2 alum treatment zones.

Fig. 25. Vertical profiles in water temperature, dissolved oxygen, and total phosphorus (P) on 20 July and 3 August 2020. Blue shaded area denotes the 25 -ft depth zone proposed for the third partial Al treatment in 2021.